Supplementary material

Nanostructured electrically conductive hydrogels via ultrafast laser processing and self-assembly

By Yufeng Tao*, Chengyiran Wei, Chunsan Deng, Jingwei Liu, Song Cai and Wei Xiong*

[*] Y.F. Tao, W. Xiong

E-mail: wsnwp520@sina.com, weixiong@hust.edu.cn

Wuhan National Laboratory of Optoelectronics, Huazhong University of Science and Technology, 1037 Luoyu Road, Wuhan, 430074, China;

Table of Contents

1. Cover figure of this manuscript

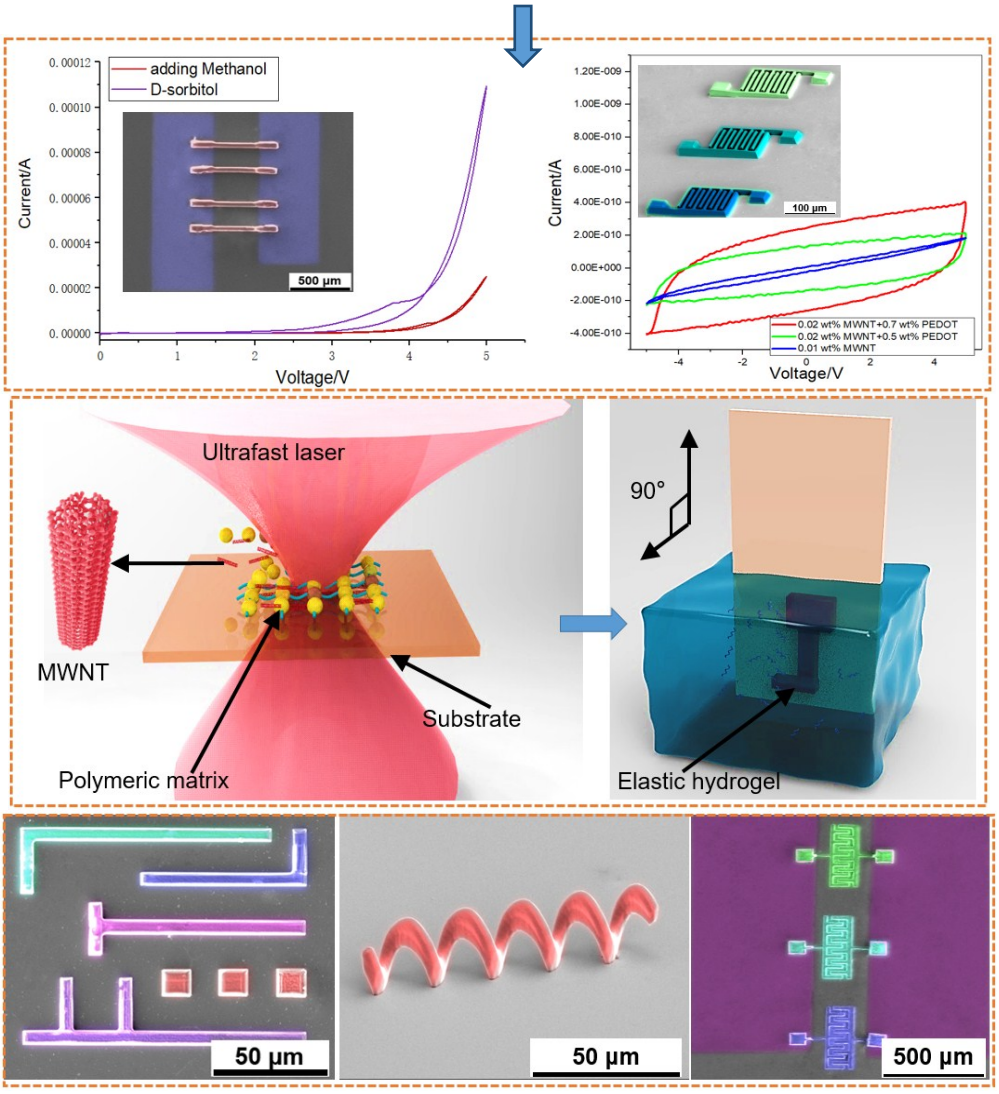

Figure S1. This manuscript introduces our work about ultrafast laser processing MWNT/polymer composite materials for absorbent polymeric matrix and self-assembly of PEDOT for multi-functional nanostructured electrically conductive hydrogels.

We adopted PEG grating to functionalize MWNTs through strong amido bonding at molecule level to improve MWNTs' dispersion, solubility and biocompatibility. Methylthionine

chloride (two-photon initiator, optical power threshold as low as 1 mW), PEG-DA (cross-linker), PEG-MWNT (conductive nanomaterials and nano sorbent), trimethylolpropane tetraacrylate (Di-TMPTTA, monomer), and AC (monomer) were mixed in ethanol as photon curable MWNT/polymer composite photoresist due to their easy radical cross-linking and miscibility. [S1]

As schematically illustrated in Figure S1, the nanofabrication contains chemistry-physics procedures: TPH on the homemade, monomeric MWNT/polymer photoresist and self-assembly of highly-conductive polymer (solution-processed PEDOT). We established an ultrashort laser system for precise localization of laser energy in space to trigger fast cross-linking reaction. A high-speed galvanometer mirror co-works with Z-axis piezoelectric ceramic translation stage to spatially moved linearly-polarization femtosecond laser beam (100 fs pulse width, tunable wavelength of 760 - 855 nm, and repetition rate of 80 MHz) inside photoresist at nanometer step (< 2 nm) to form the MWNT-embedded NECHs (Figure 1a). Mild intensity density (<15 mW/μm^2), fast scanning speed (>300 μm/s) and relatively low concentration of MWNTs (< 0.32 wt%) were optimum parameter to confine voxel for ultrafine resolution, other parameters caused unwanted aggregation of MWNTs and explosion to devastate formation quality.

Practical size of NECHs depended on the field range of microscope, movable range of z-axis of 3D platform and the maximum scanning angle of the fast-speed 2D galvanometer (intelliSCAN III 140, SCANLAB) into a rectangle area of 300 × 300 × 90 μm^3, and best spatial resolution reached 300 nm (after development) and 400 nm (after being interpenetrated by PEDOT:PSS) respectively.

2.Conductivity of the existing electrically conductive hydrogels

Although pure conductive polymers have high electrical conductivity in bulky state, but they usually lose conductivity in stepwise polymerization, 3D printing, lithographic patterning, undercut etching or sol-gel formation due to insulting organic matters blocking the continuous electron transport path or damage molecular structure of conductive polymers. Pure electronic polymers (polyaniline, polypyrrole, polythiophene, PEDOT, and other newly chemically-synthetic polymers) exhibit different-level electronic conductivity. In practice, conductive polymers were often fabricated at low purity (Aniline was polymerized with non-conductive organic crosslinking agents, [20] forming a porous structure instead of a pure bulk structure with continuous electron transport path. For example, pure PEDOT provides conductivity as high as 4000 Sm^{-1}, but will decrease to less than 1 Sm^{-1} after solution-process, where organic solvent the dopant reduced the electronic conductivity.[13]).

Most of the existing composite conductive hydrogels (PANI, PPy, PANI/folic acid), biological tissues [S3] and hemicellulose hydrogels [S7] have conductivity inferior to our work (Table1). [S3-S8] Exceptionally, some works also concluded high conductivity by rapid thermal annealing (PEDOT turns into semi-crystal state, [S4] which was a half crystalline substance with high-density electron transport path), or by the outside depositing metal Cu for metal's conductivity. [S9] As demonstration of other previously, hydrogels electronics, we listed a table containing their used materials, conductivity and the referred document.

Table1. Conductivity of the existing electric hydrogels

Material	Conductivity	Reference
PPy/PNIPAM	<0.8 Sm^{-1}	20/S2
PANI hydrogel crosslinked by phytic acid	<11 Sm^{-1}	20/S2
PNIPAM/graphene	0.7–10 Sm^{-1}	S5
PANI/folic acid	5×10^{-10}– 1.4×10^{-3} Sm^{-1}	S6

Hemicellulose hydrogel/aniline pentamer	9.05×10^{-7}–1.58×10^{-4} Sm^{-1}	S7
Tetraaniline/PVA	0.001 Sm^{-1}	20/S2
Biological tissue	0.1 to 1 Sm^{-1}	S3
Polymer/Cu metal	$>5\times10^{6}$ Sm^{-1}	42/S8
Conductive nanocomposite hydrogel	0.27 Sm^{-1}	S9
Pure PEDOT:PSS	4000 Sm^{-1}	13/S4
Our NECHs	0.05 to 42.5 Sm^{-1}	This work

3. Cross-linking reaction during TPH process

The photon-induced cross-linking reaction during TPH is similar to traditional free radical-initiated polymerization process. To clarify the reaction, we add a group of 3D molecular models in supplementary materials, and the radical cross-linking reaction now is explained as three sequential and transient reactions inside the fabrication volume. In chemistry view, the photon-induced cross-linking reaction during TPH is similar to traditional free radical-initiated polymerization process. To clarify the reaction, we add a group of 3D molecular models in supplementary materials (Figure S2), and the radical cross-linking reaction is explained as:

(1) Photolysis: Photolysis of the photon initiator to structural decompose out the free radicals. Methylthionine chloride simultaneously absorbs energy of two photons to structural decomposed, releasing benzene ring radicals (R·) as photolysis. Two-photon excitation of MC at near-infrared wavelength easily happens by the high instantaneous peak power of ultrafast laser pulses, and radicals fast diffuse in liquid-state photoresist. Probability of two-photon absorption is proportional to the square of the laser power during TPH:

$$dW/dt = 8\pi^2\omega\pi P^2 Im(\chi^3)/n^2c^2, \quad (1)$$

$$N = \eta(dW/dt), \quad (2)$$

where W denotes the absorbed photon energy, ω denotes optical frequency, n is the refraction index of the photoresist, c is the speed of light in vacuum, I is the laser power, $Im(\chi^3)$ denotes the imaginary part of the nonlinear polarization, N denotes the radical density related to the two-photon absorption ratio, η, which is a coefficient determined by the material and voxel volume.

(2) Photo-initiation: When free radicals accumulated over the threshold value, they extracts hydrogen atoms from the monomeric or low-polymeric materials, turning them into the transitional, excited state. In the case, the cross-linker PEG-DA (having double acrylate bonding), and Di-TMPTTA (having triple acrylate bonding) are easily to initiate, the AC is monomeric material for high-level polymerization. Free radicals extract hydrogen atoms from AC, PEG-DA, Di-TMPTTA to generate transitional radicals ($a\cdot$, $b\cdot$ and $c\cdot$).

$$MC \xrightarrow{hv+hv} MC^* \rightarrow R\cdot + R\cdot + \ldots \quad (3)$$

$$\begin{cases} R\cdot + (AC) \rightarrow a\cdot \\ R\cdot + (PEG-DA) \rightarrow b\cdot \\ R\cdot + (Di-TMPTTA) \rightarrow c\cdot \end{cases} \quad (4)$$

(3) Cross-linking: C=C double bonding of DA groups of the used acrylate materials begin to cleave after radicals concentrated at threshold value and randomly links with the sounding radically-initiated monomeric materials, the carbon bonding of different materials finally cross-links with each other, forming a hybrid, polymeric network. Transitional radicals randomly cross-link with remnant monomers to construct a highly linked network until all radicals are consumed.

$$a\cdot + b\cdot + c\cdot + (AC)_n + (PEG-DA)_m + (Di-TMPTTA)_k \rightarrow abc(AC)_n(PEG-DA)_m (Di-TMPTTA)_k \quad (5)$$

Asterisk (*) denotes the excited state of initiated materials, and subscripts *n*, *m* and *k* were random integers, depending on the dispersity of all kinds of monomers, the viscosity of the photoresist, and the energy distribution of the laser beam. For a standard 780 nm ultrafast laser pulse (100 fs pulse duration, 80 MHz repetition rate), the TPH voxels has an ellipsoidal cross-section with a height of 850 ± 100 nm and a width of 280 ± 80 nm. MC molecules absorbs two photons from a mild power of 1.5~20 mW. A higher laser power (30-60 mW) damages the stimuli-responsive functional groups. An excessive power (> 65 mW) ablates the hydrogel. Suitable scanning speeds varies from 10 to 2050 μm/s. TPH on composite materials promises a spatial resolution beyond the optical diffraction limit similar to conventional two-photon polymerization (TPP) on acrylate materials.

The photochemical hypothesis is described as chain-style reactions to explain interactions of stimuli-responsive monomers under ultrafast laser irradiation in the three transient reactions. Specially, the dispersed PEG-MWNTs aggregate in cross-linking reaction around the laser focus by the local gradient stress from optical tweezer effect, and embedded in polymeric matrix. The Raman spectrum of Figure 1 in some extent reveals in the cross-linking reaction.

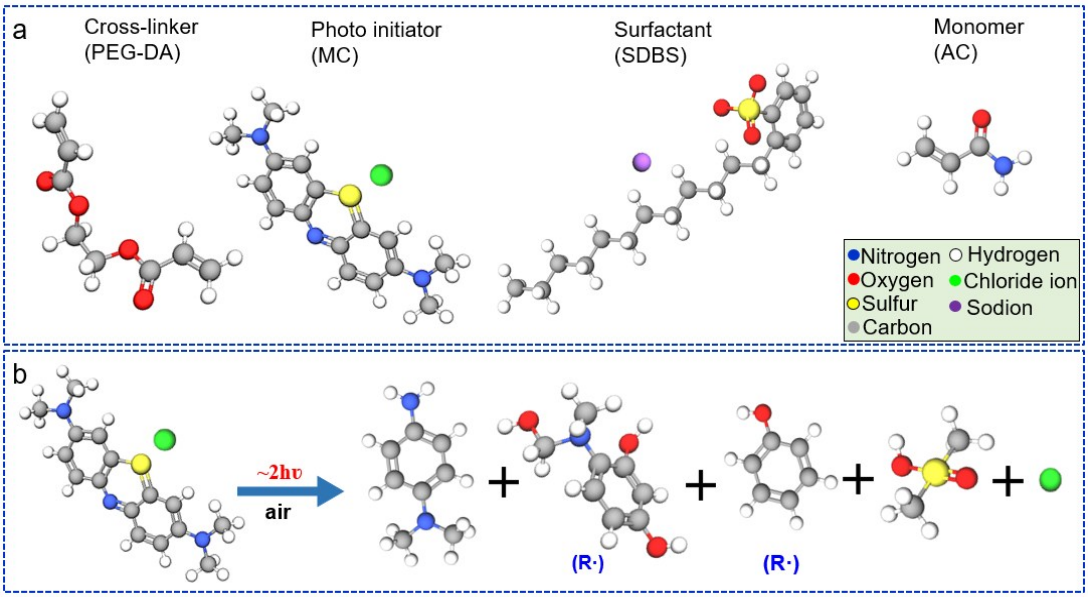

Figure S2. Molecular models of (a) used materials (PEG-DA, MC, SDBS, AC), (b) Photolysis process of MC by two-photon absorption.

4. Resistance measurement of PEDOT film

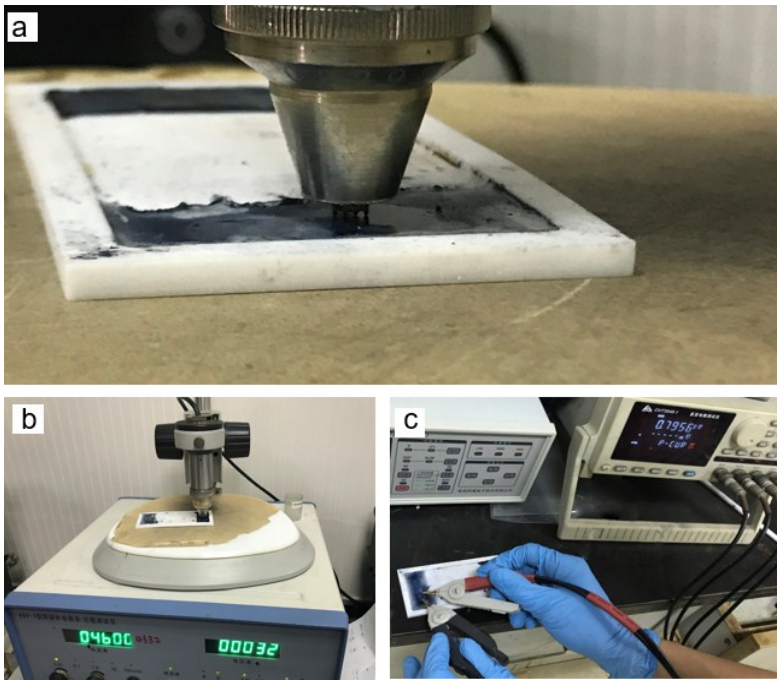

Figure S3. (a) Zoomed-in picture of four probes testing on a PEDOT/MWNT film (5 wt% methanol, 0.01 wt% MWNTs) in a polytetrafluoroethylene groove. (b) Overview of the Four probes resistance testing. (c) PEDOT film was also measured using a direct-current resistance meter, resistance value is 0.7956 KΩ.

Average thickness (*d*) of PEDOT film is about 1 μm, tester (KQY-1, Jingge electronics) gave the sheet resistance (*Rs*), 32 Ω/sq. Electrical conductivity σ is calculated following the formula, which is approximately 0.312 Sm^{-1}.

$$\sigma = 1/(Rs \times d) \tag{6}$$

5. Conductivity measurement of NECHs under different ratio ethanol

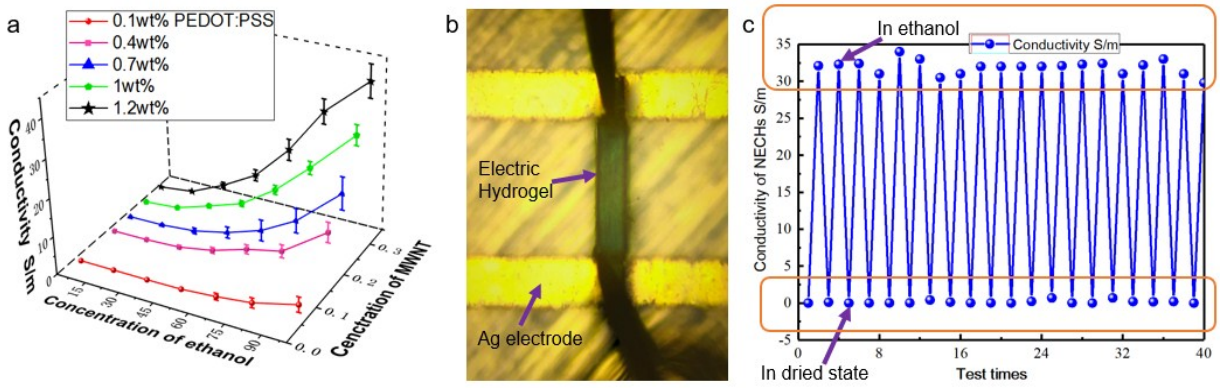

Figure S4. (a) The summarized electrical conductivity of NECHs immersed in different ratio ethanol. (b) Phone picture of the NECHs testing in advanced parameter analyzer. (c) A group of testing conductivity of NECHs in "immersed state"-to-"dried state".

We fabricated a batch of cuboid hydrogels (three dimension of 3×50×400 μm^3) bridging Ag electrodes at different MWNTs concentration. Commercial PEDOT:PSS solution (1.4 wt%) and 99.9% purity ethanol are diluted with deionized water (resistance >18 MΩ)

respectively. The measured results are calculated via Equation (6) and summarized in Figure S4. A group of repeated test of conductivity is performed on the hydrogel in dried and swelled state.

6.Observation of PEG-grating on MWNTs

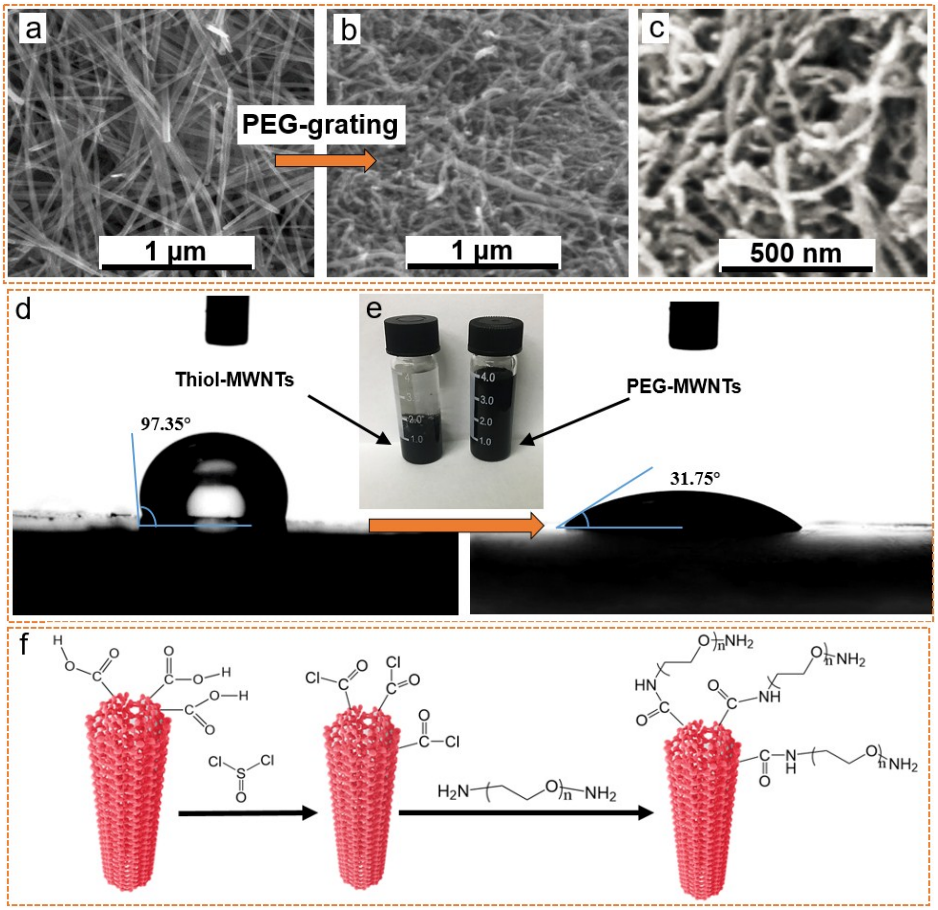

Figure S5. (a) Pure MWNTs without surface modification.[S2,S10] (b) The bulk-aggregated PEG-MWNTs and zoomed-in view (c). (d) Dynamic water contact angles of Thiol-MWNTs and PEG-MWNTs films, which are vacuum filtrated form micrometer thickness film. (e) Two bottles of water solution contains Thiol-MWNTs and PEG-MWNTs respectively, both of which are placed over two nights.(f) Chemical expression of PEG-grating.

Bio-compatable grating method contains two steps: 1. Acyl chlorination reaction. 2. PEG-grating by amido bonding. The PEG-modified MWNTs show much higher water solubility and achohol solubility than carboxyl or hydroxyl functionalized CNTs. SEM images shown the MWNCTs before and after PEG-functionalization, [S2,S10,S11] and no sediment/aggregation is found after long-term shaking or placing over five days.

7. Molecule structure of PEDOT:PSS

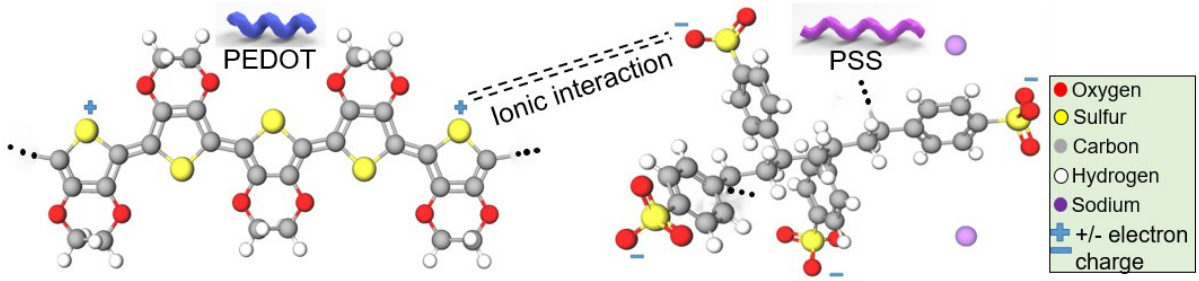

Figure S6. Molecule structure of (a) PEDOT: (b) PSS.

8. Interaction between of PEDOTs and MWNTs

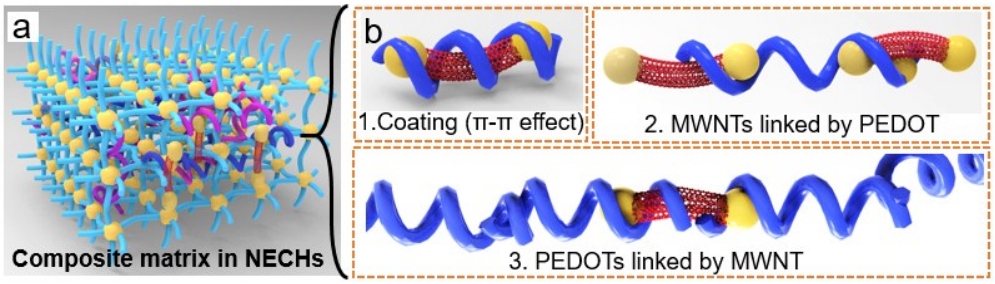

Figure S7. (a) The hybrid polymer/MWNT/PEDOT/PSS matrix, (b) Three interaction ways between PEDOT and MWNTs.

Inside the interpenetrated, hybrid, polymeric network of PEDOT/PSS/MWNT/polymer, PEDOT intersected with MWNT at nanoscale: 1.PEDOT coated MWNT like soft encapsulation. 2. PEDOT long chain twined round the isolated MWNTs for continuous electron charge transport. 3. MWNT connected the folded PEDOT chains as carbon bridge. MWNT/PEDOT intersection constructed a continuous transport path for electron, leading to high electron mobilization inside percolation network. The carbon/organic hydrogels maintained the user-customized 3D nanostructures and ultrahigh spatial resolution in our surface characterization.

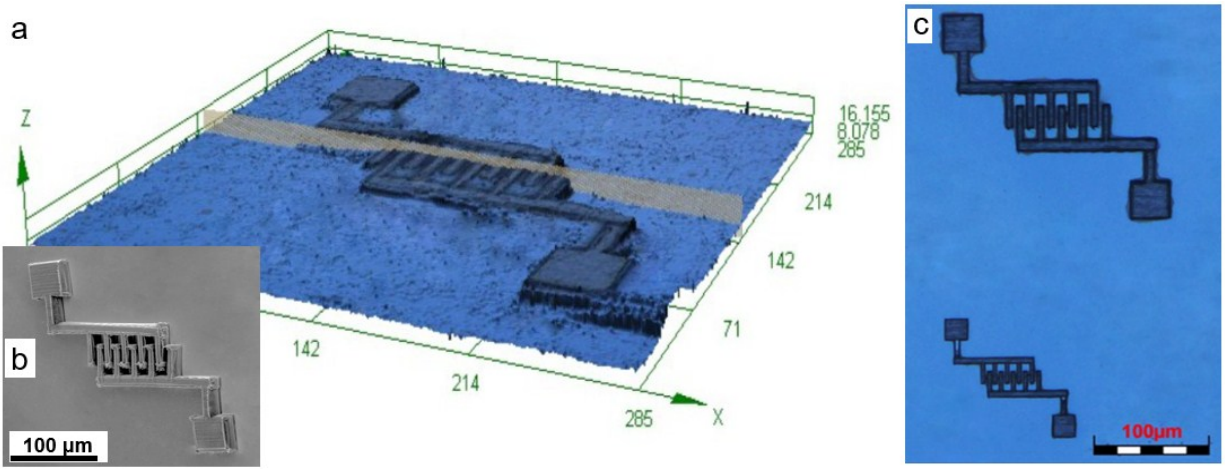

9. 3D Micrograph of the in-plane NECH capacitors

Figure S8. 3D Micrograph of the in-plane ultrathin capacitor [S12,S13] taken by LEXT-OLS 5000 of Olympus, (a) 3D profile of NECH, height < 3.5 µm, the inserted (b) is its corresponding SEM image, (c) Top view of different size NECHs.

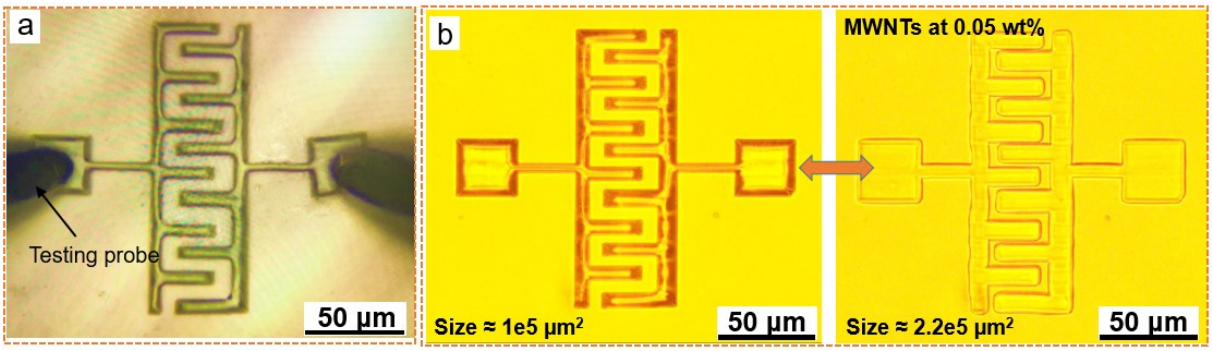

10. Swelling-up of MIC by PEDOT solution

Figure S9. (a) MIC directly-touched by probes in electrical test. (b) Reversible swelling of MIC (MWNT concentration of 0.05 wt%) in diluted PEDOT solution (Video movie, supplementary material).

We artificially set a spacing between the serpentine scanned path to loosely cross-link polymers, therefore guaranteed a high hygroscopic swelling (swelling ratio exceeds 200 %, Video-1) for water diffusion and better loading PEDOT:PSS. Hybrid matrix rendered NECHs with a disorderly-folded, half-interpenetrated architecture, providing large free volume for self-assembly of PEDOTs.

11. SEM images of surface morphology of MIC

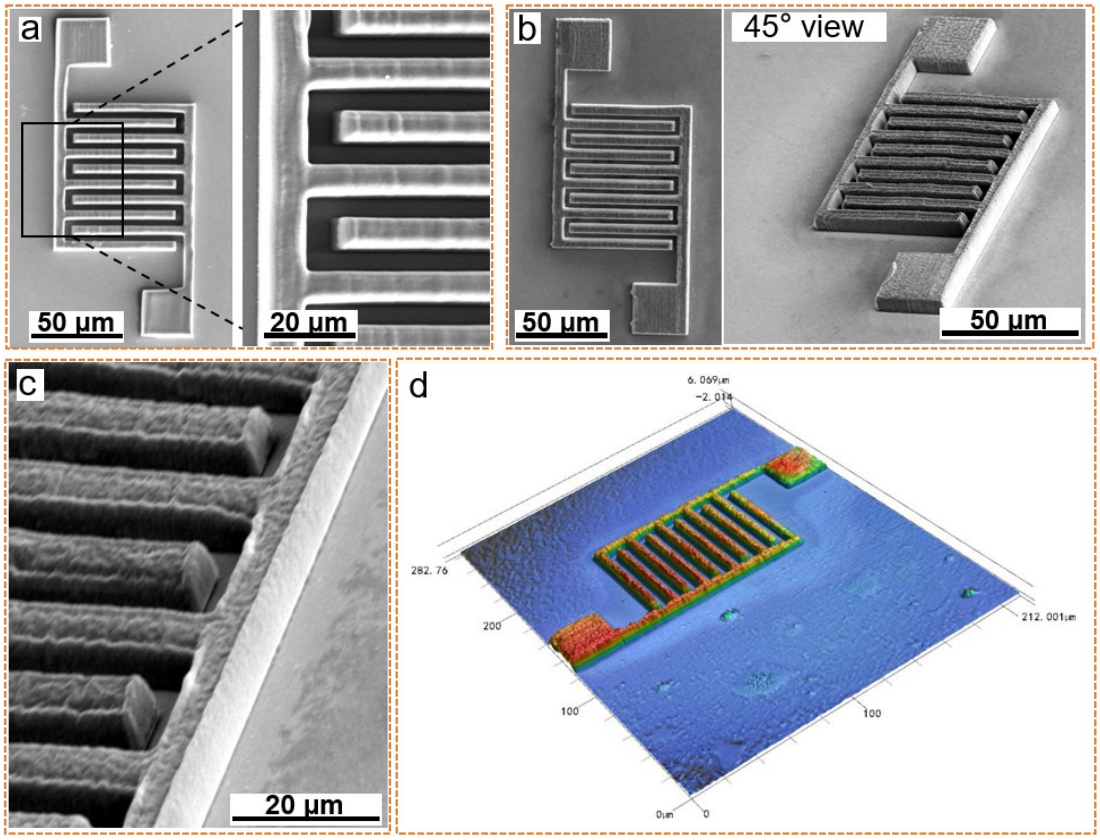

Figure S10. SEM images of MIC before and after immersion in PEDOT:PSS solution. (a) MIC fabricated by TPH with a relatively smooth surface.(b) The same MIC after 30

min PEDOT solution immersion. (c) Magnified surface of PEDOT-processed MIC.(d) 3D micrograph by VK-X1000 of KENYENCE, presenting an amorphous, wrinkled surface.

12. Edx of NECHs

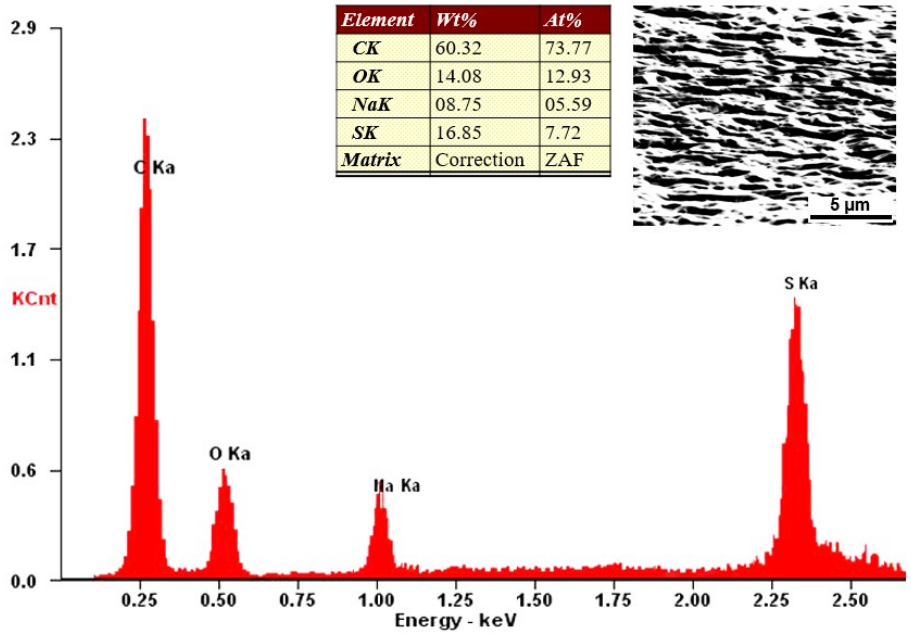

Figure S11. EDx analysis of surface of the PEDOT-interpenetrated hydrogels. At% denotes atom weight. Sulfur and Sodium are contributed by PSS and SDBS.

References

[S1] C.Y. Wang, K.L. Xia, H.M. Wang, X.P. Liang, Z. Yin, Y.Y. Zhang, Advanced Carbon for Flexible and Wearable Electronics, *Adv. Mat.* 2018, 1801072

[S2] Y.Shi, C. Ma, L. Peng, G. Yu, Conductive "Smart" Hybrid Hydrogels with PNIPAM and Nanostructured Conductive Polymers. *Adv.Funct.Mater.* 2015, 25(8),1219-1225

[S3] H. W. Yuk, B. Yang, Lu, X. H. Zhao, Hydrogel bioelectronics, *Chem. Soc. Rev,* 2018, 10.1039/C8CS00595H

[S4] B. Y. Lu, H.W. Yuk, S.T. Lin, N.N Jian, K. Qu, J.K. Xu, X.H. Zhao, Pure PEDOT:PSS hydrogels, *Nat. Comm.* 2019,10, 1043

[S5] Y. D. Liu, H. J. Choi Recent progress in smart polymer composite particles in electric and magnetic fields, *Polym. Int.* 2013, 62, 147

[S6] C. Priyadarshi, B. Partha, R. Bappaditya Roy, and Arun K. Nandi, Improved Mechanical and Electronic Properties of Co-assembled Folic Acid Gel with Aniline and Polyaniline, *ACS Appl. Mater. Interfaces,* 2014, 6 (5), 3615–3622

[S7] W.F.Zhao, L. Glavas, K. Odelius, U. Edlund, A. Albertsson, Facile and Green Approach towards Electrically Conductive Hemicellulose Hydrogels with Tunable Conductivity and Swelling Behavior, *Chem. Mater.*, 2014, 26 (14), 4265–4273

[S8] S. Lee, M. Wajahat, J.H. Kim, J. Pyo, W. S. Chang, S. H. Cho, J.T. Kim, S. K. Seol, Electroless Deposition-Assisted 3D Printing of Micro Circuitries for Structural Electronics, *ACS Appl. Mater. Interfaces.* 2019, 11 (7), 7123-7130

[S9] M.Wang, Y.J Chen, ,R. Khanc,H. Z. Liu, ,C. Chen,T. Chen, R.J Zhang ,H. Li A fast self-healing and conductive nanocomposite hydrogel as soft strain sensor. *Coll. Surf. A.* 2019, 567, 139-149

[S10] S. Gong, W. Cheng, One-Dimensional Nanomaterials for Soft Electronics, *Adv. Electron. Mater.* 2017, 3, 1600314

[S11] Y.Wang, Chenxin Zhu, R. Pfattner, H.P. Yan, L.H. Jin, S.C. Chen,F. Molina-Lopez, F. Lisse, J. Liu, N. Rabiah, Z. Chen, J. W. Chung, C. Linder, M.F. Toney, B. Murmann, Z.N Bao, A highly stretchable, transparent,and conductive polymer. *Sci.Adv.* 2017, 3, e1602076

[S12] N.H. Liu, Y.H Gao, Recent progress in micro-supercapacitors with in-plane interdigital electrode architecture, *Small*. 2017, 1701989

[S13]K. Wang, L. Tian, T.H. Wang, Z. Q. Zhang, X.J. Gao, L. Wu, B. Fu, X.H. Liu, Electrodeposition of alginate with PEDOT/PSS coated MWCNTs to make an interpenetrating conducting hydrogel for neural interface, *Compos. Interfaces.* 2019,26(1), 27–40